**Microstructures**

**Research Article**

# Grain engineering of high energy density BaTiO₃ thick films integrated on Si

**Jun Ouyang[1,2,3]** (iD) **, Xiaoman Teng[1], Meiling Yuan[3,4], Kun Wang[3,5], Yuyao Zhao[3], Hongbo Cheng[1,3], Hanfei Zhu[1,3], Chao Liu[1], Yongguang Xiao[2], Minghua Tang[2], Wei Zhang[3,6], Wei Pan[7]**

[1]Institute of Advanced Energy Materials and Chemistry, Jinan Engineering Laboratory for Multi-Scale Functional Materials, School of Chemistry and Chemical Engineering, Qilu University of Technology (Shandong Academy of Sciences), Jinan 250353, Shandong, China.
[2]Key Laboratory of Key Film Materials & Application for Equipment, School of Material Sciences and Engineering, Xiangtan University, Xiangtan 411105, Hunan, China.
[3]Key Laboratory for Liquid-Solid Structure Evolution and Processing of Materials (Ministry of Education), School of Materials Science and Engineering, Shandong University, Jinan 250061, Shandong, China.
[4]Academic Affairs Office  Civil Aviation University of China, Tianjin 300300 China.
[5]China Tobacco Shandong Industrial Co., Ltd., Jinan 250014, Shandong, China.
[6]College of Electronic and Optical Engineering, Nanjing University of Posts and Telecommunications, Nanjing 210023, China.
[7]State Key Laboratory of New Ceramics and Fine Processing, Tsinghua University, Beijing 100084, China.

**Correspondence to:** Prof./Dr. Jun Ouyang, School of Chemistry and Chemical Engineering, Qilu University of Technology, #3501 Daxue Road, Jinan 250353, Shandong, China. E-mail: ouyangjun@qlu.edu.cn

## Abstract

Ferroelectric (FE) ceramics with a large relative dielectric permittivity and a high dielectric strength have the potential to store or supply electricity of very high energy and power densities, which is desirable in many modern electronic and electrical systems. For a given FE material, such as the commonly-used BaTiO₃, a close interplay between defect chemistry, misfit strain, and grain characteristics must be carefully manipulated for engineering its film capacitors. In this work, the effects of grain orientation and morphology on the energy storage properties of BaTiO₃ thick films were systematically investigated. These films were all deposited on Si at 500 °C in an oxygen-rich atmosphere, and their thicknesses varied between ~500 nm and ~2.6 μm. While a columnar nanograined BaTiO₃ film with a (001) texture showed a higher recyclable energy density $W_{rec}$ (81.0 J/cm³ *vs.* 57.1 J/cm³ @3.2 MV/cm, ~40% increase) than that of a randomly-oriented BaTiO₃ film of about the same thickness (~500 nm), the latter showed an improved energy density at a reduced electric field with an increasing film thickness. Specifically, for the 1.3 μm and 2.6 μm thick polycrystalline films, their energy storage densities $W_{rec}$

reached 46.6 J/cm$^3$ and 48.8 J/cm$^3$ at an applied electric field of 2.31 MV/cm (300 V on 1.3 µm film) and 1.77 MV/cm (460 V on 2.6 µm film), respectively. This ramp-up in energy density can be attributed to increased polarizability with a growing grain size in thicker polycrystalline films and is desirable in high pulse power applications.

**Keywords:** Energy storage, ferroelectric, grain engineering, BaTiO$_3$, film capacitors, Si

## INTRODUCTION

With the development of various energy-harvesting technologies and associated applications, devices that can provide both high-density storage and rapid electricity supply have become increasingly important. Dielectric capacitors using ferroelectric (FE) ceramics with a high relative dielectric permittivity have demonstrated such a potential[1-5]. However, there are compromises that hinder the further development of FE ceramic capacitors for energy storage applications. These compromises include complex compositions, high composition sensitivity, and high processing temperatures, which are especially challenging for integrated film capacitors[6-8]. Therefore, the development of simple composition FE film capacitors with a high energy density, such as BaTiO$_3$, has become an emergent challenge for the future of electric energy storage using dielectric capacitors.

Once a manufacturable composition was selected, the performance of FE film capacitors was mostly affected by the substrate, which imposes a clamping effect[9] and a residual strain[10], the deposition chemistry[11], and the crystalline or grain characteristics[12,13]. These factors are usually intertwined, and hence it is difficult to separate out their contributions to the energy storage performance of the film. In this work, we chose the prototype FE of BaTiO$_3$ for its simple composition and broad application in electro ceramics, especially ceramic capacitors. Established deposition chemistry, i.e., sputtering deposition in an oxygen-rich atmosphere, was used for the preparation of BaTiO$_3$ film capacitors on a Si substrate[13]. Therefore, in this work, we were able to focus on the grain effects on the energy storage performance of the FE film capacitors, including the effects of grain orientation and grain morphology.

Our previous investigations on preparing high energy density BaTiO$_3$-based film capacitors[13-15] have focused on a columnar nanograin design via a low-temperature process (350-400 °C) and a buffer-layer technique. This approach resulted in a densely-packed nanograin array, which shows a (001)-texture, an in-plane grain diameter down to 10-20 nm, and a grain length extending through the thickness of the film. Due to periodic gradients in the electric polarization and relative dielectric permittivity, the total dielectric displacement of such a film is confined and experiences a significantly delayed saturation under an external field. Consequently, such a grain structure is endowed with a high breakdown field and a large energy storage density. For example, a recyclable energy density of ~130 J/cm$^3$ at ~650 MV/m[13] and ~229 J/cm$^3$ at 875 MV/m[15] was achieved in columnar-grained BaTiO$_3$ films of ~350 nm and ~160 nm thick, respectively. However, these high energy densities were achieved under very large electric fields, corresponding to a much-reduced relative dielectric permittivity. This is not always the optimum solution for the storage and/ or supply of electric energy, especially in cases where high pulsed power is demanded under middle-to-low electric fields.

In this work, we aimed to manipulate the grain characteristics, including grain orientation and morphology, to achieve a high energy density at a reduced electric field in BaTiO$_3$ film capacitors. To achieve this goal, a higher growth temperature at 500 °C was used, and a compromise was made between improved crystallinity, which enhances the dielectric response, and increased average grain size, which reduces the

maximum applicable electric field. By using a thick $LaNiO_3$ buffer layer (~110 nm) on platinized Si and a fast deposition rate, we successfully suppressed the growth of randomly-oriented, discontinuous columnar grains in the $BaTiO_3$ film directly deposited on the Pt electrode. Instead, we achieved a (001)-textured, continuous columnar nanograin structure. This structure is similar to those obtained at low deposition temperatures[9,10] but with an increased average grain size (~50-60 nm *vs.* 10-20 nm), resulting in an enhanced dielectric response. In comparison to the unbuffered films, the $LaNiO_3$-buffered $BaTiO_3$ films exhibited a higher dielectric polarization under the same applied electric field (320 MV/m), leading to a ~40% boost in the recyclable energy density of a film capacitor (81.0 $J/cm^3$ *vs.* 57.1 $J/cm^3$ @3.2 MV/cm). Furthermore, to break down the aspect-ratio conservation of the continuous columnar nanograin microstructure and its associated thickness scalable energy storage performance[13], we went back to the classic random polycrystalline $BaTiO_3$ film directly deposited on platinized Si. The rapid growth of its grain size with deposition time led to an increasing polarizability/relative dielectric permittivity with the film thickness. Consequently, an enhanced energy storage density close to 50 $J/cm^3$ was achieved in device-level thick $BaTiO_3$ films (46.6 $J/cm^3$ @300 V on a 1.3 μm thick film and 48.8 $J/cm^3$ @460 V on a 2.6 μm thick film). These values are ~25 times higher than those of the $BaTiO_3$ ceramics and serve as an important benchmark for the future development of multilayer ceramic capacitors (MLCCs).

## MATERIALS AND METHODS

For the preparation of the platinized Si substrate, a Pt/Ti bilayer bottom electrode was used. The Ti layer, with a thickness of ~10 nm, is the adhesion layer to bond with the Si substrate. The deposition process was carried out on a (100) Si substrate at 300 °C via dc magnetron sputtering in a pure Ar atmosphere. The resulting Pt layer showed a high degree of (111) texture. It is noteworthy that these platinized Si substrates are also commercially available for this purpose. The (100) Si substrates (10 mm × 10 mm) and ceramic targets of $BaTiO_3$ and $LaNiO_3$ (Φ = 50 mm, t = 5 mm, 99.9% purity) were purchased from the Anhui Institute of Optics, Chinese Academy of Science. The Pt and Ti sputtering targets (Φ = 50 mm, t = 3 mm, 99.99% purity) were purchased from Zhongnuo Advanced Material Technology Co. Limited (Beijing, China). The key deposition parameters of the $LaNiO_3$-buffered and unbuffered $BaTiO_3$ film heterostructures are summarized in Table 1. Dot-shaped Au top electrodes (Φ = 0.2 mm) were sputtered through a masked plate at room temperature for electrical measurements.

The microstructure of the two types of $BaTiO_3$ thin film heterostructures was characterized by using X-ray diffraction (XRD) $\theta$-$2\theta$ scans in a commercial Rigaku Dmax-rc XRD diffractometer equipped with a Ni-filtered Cu K radiation source. The surface morphologies were analyzed via atomic force microscopy (AFM) on a MicroNano D-5A scanning probe microscope (Shanghai, China). The layer thicknesses and nanostructures of the $BaTiO_3$ thin film heterostructures were analyzed via transmission electron microscopy (TEM) using a JEM-2010 microscope (JEOL, Japan). The room temperature FE hysteresis loops (P-V) were measured at 100 Hz via a commercial Multiferroic™ FE tester (Radiant Technology, USA). The voltage-dependent capacitance (C-V) curves, from which the relative dielectric permittivity and loss tangent as functions of the applied voltage/field were obtained, were measured by using a B1505A impedance analyzer (Agilent Technologies, USA) at 5 kHz by applying a small ac signal of 50 mV. The voltage was swept from negative maximum to positive maximum and vice versa during the measurements.

## RESULTS AND DISCUSSION

Figure 1 shows the XRD $\theta$-$2\theta$ scan patterns of the $BaTiO_3$/Pt/Ti/Si [Figure 1A] and $BaTiO_3$/$LaNiO_3$/ Pt/Ti/Si [Figure 1B] thin film heterostructures, respectively. It can be clearly seen that while the unbuffered $BaTiO_3$ film showed a typical polycrystalline structure, the $LaNiO_3$ buffered $BaTiO_3$ film was (001)-textured, as reported in our previous publications[13-15]. Furthermore, the degree of crystallinity was significantly

**Table 1. Magnetron sputtering parameters of BaTiO$_3$ film heterostructures**

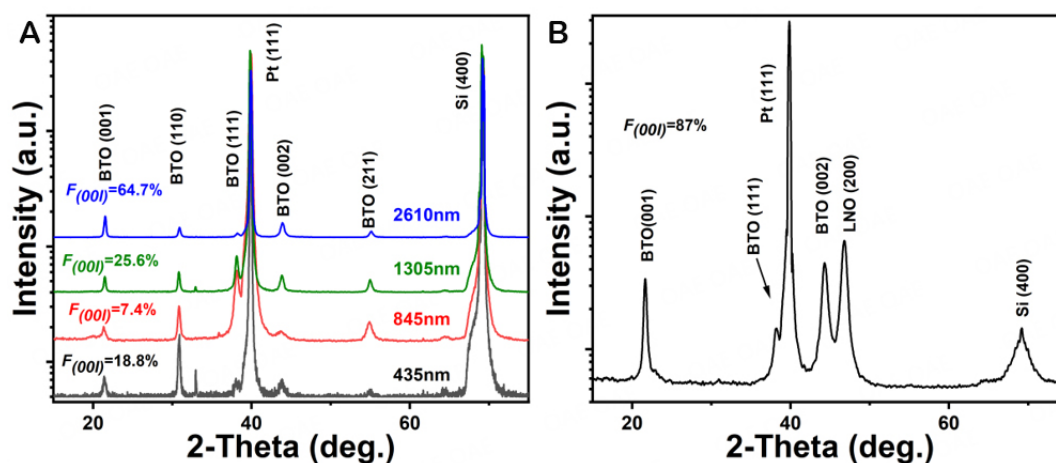| Structure type | BaTiO$_3$/Pt/Ti | BaTiO$_3$/LaNiO$_3$/Pt/Ti |
|---|---|---|
| Base pressure | $2 \times 10^{-4}$ Pa | $2 \times 10^{-4}$ Pa |
| Pt/Ti layer sputtering pressure | 0.3 Pa | 0.3 Pa |
| Pt/Ti layer thickness | ~150-200 nm | |
| Buffer layer sputtering temperature | N/A | 500 °C |
| Buffer layer sputtering atmosphere | N/A | Ar:O$_2$ (4:1) |
| Buffer layer sputtering pressure | N/A | 0.3 Pa |
| Buffer layer thickness | N/A | ~100 nm |
| BaTiO$_3$ sputtering temperature | 500 °C | 500 °C |
| BaTiO$_3$ sputtering atmosphere | Ar:O$_2$ (4:1) | Ar:O$_2$ (4:1) |
| BaTiO$_3$ sputtering pressure | 0.3 Pa | 1.2 Pa |
| BaTiO$_3$ deposition rate | ~7 nm/min | ~10 nm/min |
| BaTiO$_3$ layer thickness (nm) | 435 nm, 845 nm, 1,305 nm, 2,610 nm | 510 nm |
| Cooling atmosphere (pressure) | Pure O$_2$ (2.5 Pa) | Pure O$_2$ (2.5 Pa) |



**Figure 1.** XRD $\theta$-$2\theta$ scan patterns of the thin film heterostructures of (A) BaTiO$_3$/Pt/Ti/Si (with various thicknesses of the BaTiO$_3$ layer) and (B) BaTiO$_3$/LaNiO$_3$/Pt/Ti/Si (with a 510 nm thick BaTiO$_3$ layer).

improved in the thicker polycrystalline BaTiO$_3$ film, as evidenced by their stronger and sharper diffraction peaks. The preferred crystalline orientation, which was (110) in the 435 nm thick film, changed into (111) in the 845 nm and 1,305 nm thick films and finally became (001) in the 2,610 nm thick film. The degree of grain (00l)-orientation of unbuffered BaTiO$_3$ film was evaluated using the Lotgering factor $F_{(ool)}$ = 64.7% [Figure 1A][16] and compared with those of the standard powder XRD pattern of BaTiO$_3$ (JCPDS 05-0626). The growth of BaTiO$_3$ on (111) Pt involves a competition between various factors, including the channeling effect[17], interface energy, and surface energy. The dominance of the channeling effect is evident in the thinnest film, leading to a preferred orientation of the closest-packed plane of (110) in perovskite. As the film thickness increases, the interface energy, primarily influenced by misfit strain energy, becomes more significant. This leads to the (111) orientation, which is the best match to the (111) Pt base plane, taking over as the preferred crystalline orientation. Lastly, in the thickest film where the residual misfit approached zero, (001) crystalline planes with the minimum surface energy emerged as the preferred orientation. On the other hand, in the LaNiO$_3$-buffered BaTiO$_3$ film, since the (100)-textured growth of LaNiO$_3$ on Pt[18] has been preset, the (001) orientation of the BaTiO$_3$ film satisfies the requirement of minimum energy, which is now dominated by the interface/surface energy term. The Lotgering factor $F_{(ool)}$ for buffered BaTiO$_3$ film is
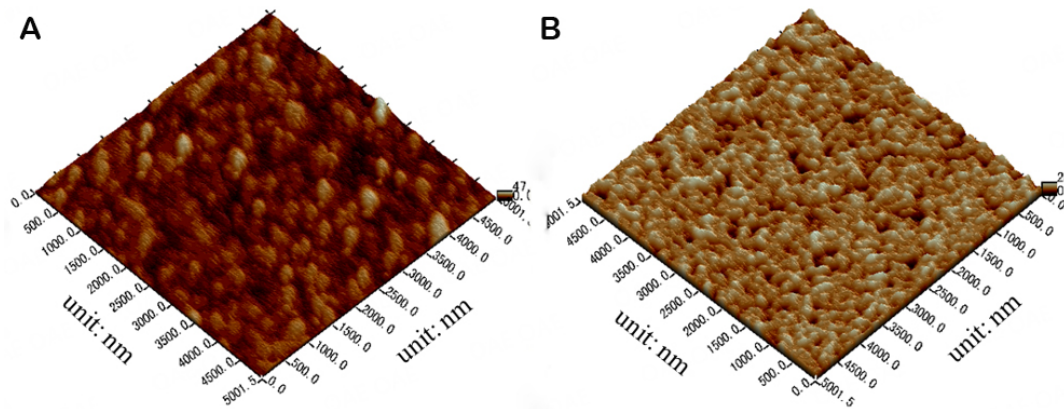
**Figure 2.** AFM surface scan images of (A) the 435 nm thick BaTiO$_3$ film grown on Pt/Ti/Si and (B) the 510 nm thick BaTiO$_3$ film grown on LaNiO$_3$/Pt/Ti/Si.
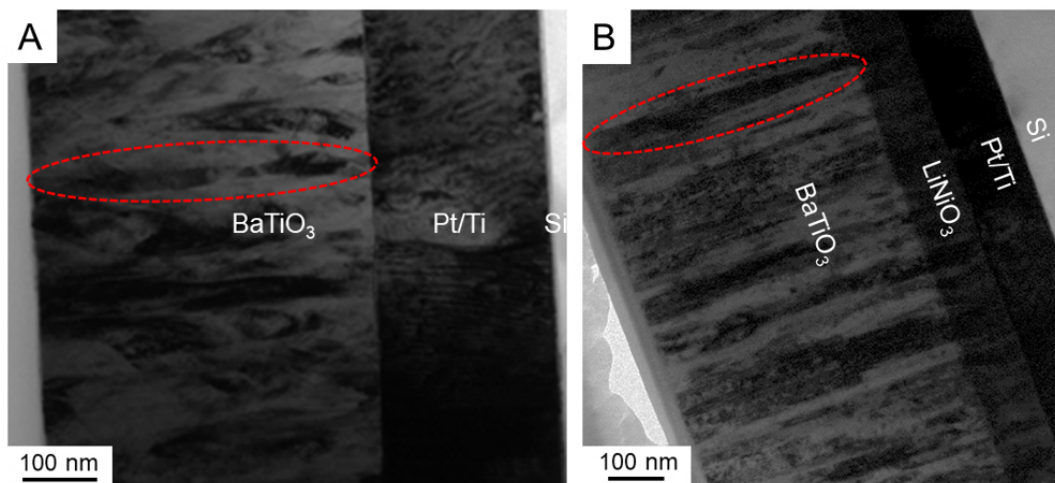


**Figure 3.** Cross-sectional TEM images of (A) the BaTiO$_3$ (435 nm) /Pt/Ti/Si and (B) the BaTiO$_3$ (510 nm)/LaNiO$_3$/Pt/Ti/Si heterostructures.

87% [Figure 1B].

According to the study by Zhang *et al.*, the relative dielectric permittivity of a polycrystalline BaTiO$_3$ film deposited on a Pt electrode[19] is expected to be higher than that of the (001)-textured film. Moreover, the presence of larger grain sizes in the thicker films warrants an improved dielectric response, which can be attributed to extrinsic sources such as domain wall movements[20] and grain re-orientations. Next, we will compare their nanostructure characteristics, including grain and interface morphologies, of the 510 nm thick buffered and the 435 nm thick unbuffered BaTiO$_3$ film samples to complement the XRD results.

Figure 2A and B displays the surface AFM image of the two films. Both films showed a dense and granular surface, with a root mean square roughness (Ra) of 2.868 (A) and 2.007 nm (B), respectively. Figure 3A and B presents the cross-sectional TEM image of the two BaTiO$_3$ films. The unbuffered film consists of discontinuous columnar nanograins, occasionally displaying twisted or canted orientations. In contrast, the bi-layer film of BaTiO$_3$/LaNiO$_3$ constitutes continuous arrays of columnar nanograins that extend from the LaNiO$_3$/Pt bottom electrode interface to the surface of the BaTiO$_3$ layer. These
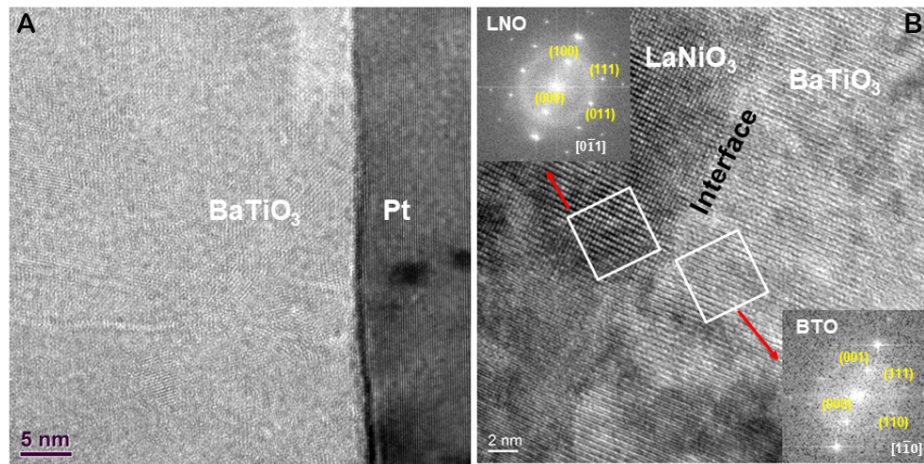
**Figure 4.** High-resolution TEM images near (A) $BaTiO_3$/Pt and (B) $BaTiO_3$/$LaNiO_3$ interfaces in the unbuffered and buffered $BaTiO_3$ film heterostructures, respectively. Insets are Fast-Fourier-Transformed (FFT) selected area electron diffraction (SAED) patterns of the local $BaTiO_3$ film and its underneath $LaNiO_3$ buffer layer.

nanostructures are characteristic of sputtered perovskite/Pt[17] and perovskite/perovskite heterostructures[13]. For the $BaTiO_3$/Pt case, the XRD analysis revealed the competition between multiple crystalline orientations, leading to a "broken" nanograin morphology with twisted/canted grain variants. In contrast, the presence of the lattice-matched, (100)-oriented $LaNiO_3$ buffer layer provides local coherency within each grain nucleus of $BaTiO_3$. This has promoted a (001)-textured, continuous growth of the columnar nanograins in the $LaNiO_3$/$BaTiO_3$ bi-layer film[13]. From TEM images, the unbuffered and $LaNiO_3$-buffered $BaTiO_3$ films showed an average grain diameter (in-plane) ~50-60 nm and ~30-40 nm, respectively. These grain sizes are much larger than those of the low-temperature deposited $BaTiO_3$ films with a superfine columnar nanograin structure[13-15], which showed a boosted energy storage density at a high field by sacrificing their relative dielectric permittivity. Therefore, these two types of $BaTiO_3$ films deposited at 500 °C are expected to show an enhanced dielectric response and boosted energy storage performance at middle-to-low electric fields.

In Figure 4, we present the high-resolution TEM images near the $BaTiO_3$/Pt (A) and $BaTiO_3$/$LaNiO_3$ interfaces in the unbuffered and buffered $BaTiO_3$ film heterostructures, respectively. The $BaTiO_3$/Pt interface exhibits a clean-cut interface with a narrow boundary layer of ~1-2 nm, indicating a limited degree of interdiffusion. This is consistent with the medium deposition temperature (@500 °C) and is supported by an elemental line scan analysis via energy dispersive spectroscopy (EDS) in a Scanning Transmission Electron Microscope. In Figure 4B, the imaged section of the $BaTiO_3$ film, located inside a single grain, showed an "atomically smooth" and locally-coherent growth on the underlying $LaNiO_3$ layer. This indicates a locally coherent or "heteroepitaxial" growth inside the grain. The Fast-Fourier-Transformation of Figure 4B led to a selected area electron diffraction (SAED) pattern that complements the XRD results. It not only verifies an out-of-plane $(001)_{BaTiO_3}//(100)_{LaNiO_3}$ crystalline correlation but also reveals an in-plane crystalline correlation of $[100]_{BaTiO_3}//(010)_{LaNiO_3}$. Overall, the high-quality surfaces and interfaces, together with the dense nanograin morphology, will contribute to a high breakdown strength and a large energy storage density of the $BaTiO_3$ films. Specifically, for the unbuffered $BaTiO_3$ films, since the grain shape is irregular and preferred grain orientation varies with film thickness, the energy storage density at a given field will be thickness-dependent. Taking into consideration that the degree of crystallinity, especially the grain size, increases with the film thickness, we would expect a higher relative dielectric permittivity in a thicker film, together with a higher energy density at a low electric field. This is due to an enhanced

"polarizability", i.e., early saturation of the electric polarization in comparison to that of the low-temperature deposited $BaTiO_3$ films.

In Figure 5A, we present typical polarization-electric field (*P-E*) hysteresis loops of the $LaNiO_3$ buffered $BaTiO_3$ film at successively increasing voltages of 100 V, 120 V, and 160 V. The *P-E* loops did not show signs of saturation until under the largest applied voltage of 160 V, at which the applied electric field approached 314 MV/m and the electric polarization reached ~75 C/cm². The recyclable energy densities $W_{rec}$ as functions of the applied electric field were computed via the integration of the *P-E* loops ($W_{rec} = \int_{P_r}^{P_{max}} E dP$)[13]. The relative dielectric permittivity $\varepsilon_r$, $\varepsilon_r = (2\int_0^P E dP)/(E^2 \varepsilon_0)$, where $\int_0^P E dP$ is the total stored electric energy under field *E*, was obtained from monopolar *P-E* loops (not shown here). Figure 5B presents the $W_{rec}$ and $\varepsilon_r$ values of the LaNiO-buffed $BaTiO_3$ along with those of a $BaTiO_3$ ceramic[21]. Under an applied maximum field of ~314 MV/m, the electric energy density $W_{rec}$ of the buffered $BaTiO_3$ film reached ~81 J/cm³, and the relative dielectric permittivity $\varepsilon_r$ ranged between 470 (@low field) and ~215 (@low field). In contrast, the maximum electric energy density $W_{rec}$ of the $BaTiO_3$ ceramic, which has the largest reported bulk dielectric strength[21], is only ~1.8 J/cm³. The $W_{rec}$-E curves of the two materials overlap fairly well at low electric fields (< ~50 MV/m), but the corresponding $\varepsilon_r$-E curves are quite different. In the $BaTiO_3$ ceramic, $\varepsilon_r$ quickly drops to ~200 at E = 30 MV/m and remains constant as the field increases until it reaches the breakdown limit of ~90 MV/m. In contrast, in the $BaTiO_3$ film, $\varepsilon_r$ gradually decreases from ~300 at *E* = 30 MV/m to ~215 at *E* ~314 MV/m, indicating a much slower saturation of the electric polarization compared to the bulk $BaTiO_3$. The grain size of $BaTiO_3$ thin films is only several tens of nanometers, which is much smaller than that of its ceramic counterpart (ranging from a few micrometers to tens of micrometers). Due to this extremely small grain size, a full polarization alignment in $BaTiO_3$ thin films becomes very difficult under an intermediate electric field (~10 MV/m). In bulk ceramics, this level of field is usually sufficient to saturate the electric polarization. However, in the nanoscale grains of the $BaTiO_3$ thin films, a field level of about one order of magnitude higher (~100 MV/cm) is required to align all accessible polarization vectors, resulting in a slow electric polarization saturation. The delayed saturation of the electric polarization enables the absorption of additional electrical energy and greatly extends the electric breakdown limit. Consequently, our $BaTiO_3$ films exhibit outstanding energy storage capacities under electric fields of several hundred MV/m.

Furthermore, the unbuffered, randomly oriented $BaTiO_3$ films (on Pt/Ti/Si) showed a distinct energy storage feature compared to the (001)-textured, $LaNiO_3$-buffered $BaTiO_3$ films. Unlike the latter, which have shown a thickness-scalable relative dielectric permittivity $\varepsilon_r$/energy density[13] by maintaining an aspect-ratio of in-plane diameter/grain length, the randomly oriented films demonstrate an increasing energy density $W_{rec}$ and $\varepsilon_r$ at a given low field with the film thickness [Figure 6A and B, Table 2]. These behaviors, as predicted by the microstructural analyses, can be attributed to the discontinuous columnar nanograin morphology with mixed crystalline orientations and the growth of these nanograins with the film thickness. It is worth noting that at a high voltage of 460 V, the 2,610 nm thick film showed a low dielectric loss (< 3%) and a high electric polarization (> 75 C/cm²). This can be attributed to its large thickness (460 V corresponding to a low field of ~117 MV/m) and good film quality/robust insulation.

## CONCLUSIONS

In summary, the study investigates the energy storage capabilities of $BaTiO_3$ thick films (~0.5 μm to ~2.6 μm) deposited at 500 °C, with two types of engineered grain structures. The films with a (001)-textured, continuous columnar nanograin structure showed a high recyclable energy density $W_{rec}$ of ~81 J/cm³ at E = 314 MV/m. This represents a substantial improvement compared to films of the same type of films

**Table 2. Energy storage densities of various BaTiO$_3$ film capacitors**

| BaTiO$_3$ thin film heterostructures sputter-deposited on Si | Applied voltage (V)/Field (MV/m) | $W_{rec}$ (J/cm$^3$) |
|---|---|---|
| Au/BaTiO$_3$ (510 nm)/LaNiO$_3$/Pt/Ti | 160/314 | 81.0 |
| Au/BaTiO$_3$ (435 nm)/Pt/Ti | 140/322 | 57.1 |
| Au/BaTiO$_3$ (845 nm)/Pt/Ti | 260/308 | 50.4 |
| Au/BaTiO$_3$ (1,305 nm)/Pt/Ti | 300/231 | 46.6 |
| Au/BaTiO$_3$ (2,610 nm)/Pt/Ti | 460/177 | 48.8 |
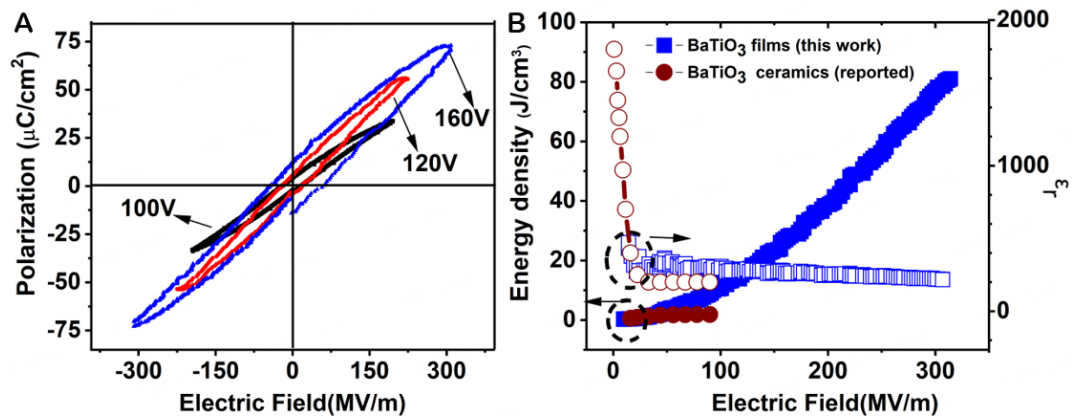


**Figure 5.** (A) Typical polarization-electric field hysteresis loops of the LaNiO$_3$ buffered BaTiO$_3$ film (~510 nm) and (B) the corresponding energy storage density $W_{rec}$ and relative dielectric permittivity of the film in (A), as well as those of a BaTiO$_3$ ceramic, plotted as functions of the applied electric field.
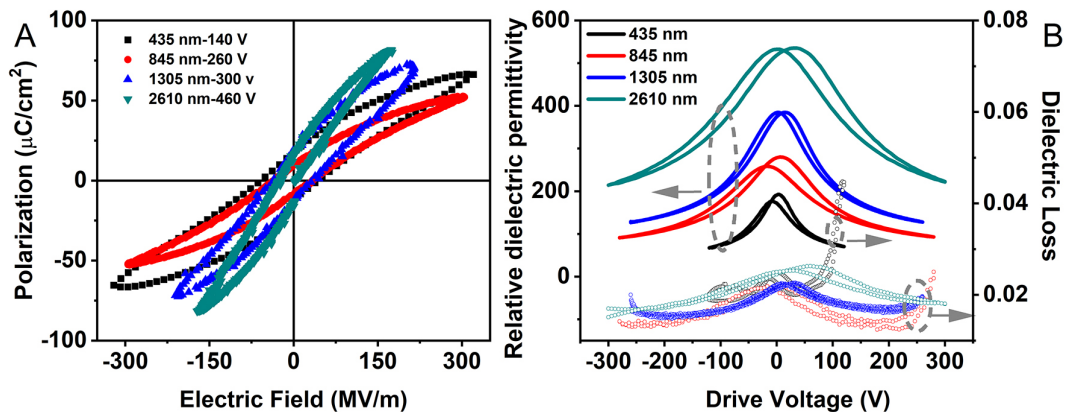


**Figure 6.** (A) Typical polarization-electric field (P-E) hysteresis loops of the four unbuffered BaTiO$_3$ films directly deposited on Pt/Ti/Si, with thicknesses ranging between 435 nm and 2610 nm; (B) The relative dielectric permittivity and loss tangents as functions of the applied voltage for the four films in (A).

prepared at lower temperatures[13-15], making them promising for energy storage under middle-to-low electric fields. Meanwhile, films consisting of discontinuous columnar nanograins with mixed crystalline orientations showed an improved relative dielectric permittivity and a higher energy storage density at low fields, with increasing film thickness. Both types of BaTiO$_3$ films have shown good potential for dielectric energy storage applications under middle-to-low electric fields. However, the randomly-oriented films are better material candidates in high-voltage applications (several times the commercially used voltage of 220 V).

## DECLARATIONS

**Authors' contributions**

Conceptualization and methodology; writing - original draft preparation: Ouyang J

Validation: Teng X, Yuan M, Wang K

Formal analysis: Yuan M, Wang K, Zhao Y, Cheng H

Investigation: Zhu H, Liu C, Xiao Y, Zhang W

Resources: Ouyang J, Tang M, Pan W

Data curation: Ouyang J, Teng X, Yuan M

Writing, review, and editing: Ouyang J, Yuan M

Visualization: Teng X, Yuan M, Ouyang J

Supervision: Ouyang J, Tang M

Project administration: Ouyang J, Pan W

Funding acquisition: Ouyang J, Cheng H, Zhu H, Liu C

All authors have read and agreed to the published version of the manuscript.

**Availability of data and materials**

Data will be available from the first author upon reasonable request.

**Conflicts of interest**

All authors declared that there are no conflicts of interest.

**Ethical approval and consent to participate**

Not applicable.

**Consent for publication**

Not applicable.

**Copyright**

## REFERENCES

1. Chu B, Zhou X, Ren K, et al. A dielectric polymer with high electric energy density and fast discharge speed. *Science* 2006;313:334-6. DOI
2. Yao K, Chen S, Rahimabady M, et al. Nonlinear dielectric thin films for high-power electric storage with energy density comparable with electrochemical supercapacitors. *IEEE Trans Ultrason Ferroelectr Freq Control* 2011;58:1968-74. DOI
3. Sigman J, Brennecka GL, Clem PG, Tuttle BA. Fabrication of perovskite-based high-value integrated capacitors by chemical solution deposition. *J Am Ceram Soc* 2008;91:1851-7. DOI

4.    Dai L, Lin F, Zhu Z, Li J. Electrical characteristics of high energy density multilayer ceramic capacitor for pulse power application. *IEEE Trans Magn* 2005;41:281-4.  DOI

5.    Chen XF, Dong XL, Wang GS, Cao F, Wang YL. Doped Pb(Zr,Sn,Ti)O$_3$ slim-loop ferroelectric ceramics for high-power pulse capacitors application. *Ferroelectrics* 2008;363:56-63.  DOI

6.    Zhu L, Wang Q. Novel ferroelectric polymers for high energy density and low loss dielectrics. *Macromolecules* 2012;45:2937-54. DOI

7.    Wang Y, Zhou X, Chen Q, Chu B, Zhang Q. Recent development of high energy density polymers for dielectric capacitors. *IEEE Trans Dielect Electr Insul* 2010;17:1036-42.  DOI

8.    Kim Y, Kathaperumal M, Smith OL, et al. High-energy-density sol-gel thin film based on neat 2-cyanoethyltrimethoxysilane. *ACS Appl Mater Interfaces* 2013;5:1544-7.  DOI

9.    Ouyang J, Yang SY, Chen L, Ramesh R, Roytburd AL. Orientation dependence of the converse piezoelectric constantsfor epitaxial single domain ferroelectric films. *Appl Phys Lett* 2004;85:278-80.  DOI

10.   Wang J, Su Y, Wang B, Ouyang J, Ren Y, Chen L. Strain engineering of dischargeable energy density of ferroelectric thin-film capacitors. *Nano Energy* 2020;72:104665.  DOI

11.   Niu M, Zhu H, Wang Y, et al. Integration-friendly, chemically stoichiometric BiFeO$_3$ films with a piezoelectric performance challenging that of PZT. *ACS Appl Mater Interfaces* 2020;12:33899-907.  DOI

12.   Su Y, Ouyang J, Zhao YY. Nanograins in ferroelectric films. In: Ouyang J, editor, Nanostructures in ferroelectric films for energy applications. Amsterdam: Elsevier; 2019; pp. 129-62.

13.   Zhao Y, Ouyang J, Wang K, et al. Achieving an ultra-high capacitive energy density in ferroelectric films consisting of superfine columnar nanograins. *Energy Stor Mater* 2021;39:81-8.  DOI

14.   Wang K, Zhang Y, Wang S, et al. High energy performance ferroelectric (Ba,Sr)(Zr,Ti)O$_3$ film capacitors integrated on Si at 400 °C. *ACS Appl Mater Interfaces* 2021;13:22717-27.  DOI

15.   Zhu H, Zhao YY, Ouyang J, Wang K, Cheng H, Su Y. Achieving a record-high capacitive energy density on Si with columnar nanograined ferroelectric films. *ACS Appl Mater Interfaces* 2022;14:7805-13.  DOI

16.   Park S, Jang J, Ahn C, et al. Buffered template strategy for improving texture quality and piezoelectric properties of heterogeneous templated grain growth (K,Na)NbO$_3$-based ceramics through interface engineering. *J Eur Ceram Soc* 2023;43:1932-40.  DOI

17.   Yuan M, Zhang W, Wang X, Pan W, Wang L, Ouyang J. In situ preparation of high dielectric constant, low-loss ferroelectric BaTiO$_3$ films on Si at 500 °C. *Appl Surf Sci* 2013;270:319-23.  DOI

18.   Wakiya N, Azuma T, Shinozaki K, Mizutani N. Low-temperature epitaxial growth of conductive LaNiO$_3$ thin films by RF magnetron sputtering. *Thin Solid Films* 2002;410:114-20.  DOI

19.   Zhang W, Cheng H, Yang Q, Hu F, Ouyang J. Crystallographic orientation dependent dielectric properties of epitaxial BaTiO$_3$ thin films. *Ceram Int* 2016;42:4400-5.  DOI

20.   Xu F, Trolier-mckinstry S, Ren W, Xu B, Xie Z, Hemker KJ. Domain wall motion and its contribution to the dielectric and piezoelectric properties of lead zirconate titanate films. *J Appl Phys* 2001;89:1336-48.  DOI

21.   Burn I, Smyth DM. Energy storage in ceramic dielectrics. *J Mater Sci* 1972;7:339-43.  DOI